

Research Article

Evaluation of antioxidant and antimicrobial action of copper nanoparticles synthesized from *Moringa oleifera* pods

Bhavani Sundar, Sankar Madhavan*

Department of Biotechnology, Rajalakshmi Engineering College, Thandalam, Chennai, India

ARTICLE INFO

Keywords:
Copper
nanoparticles
Moringa oleifera
pod
Antioxidant activity
Zone of inhibition
and antimicrobial
activity

ABSTRACT

Background: *Moringa oleifera* is a traditional South Indian medicinal plant and an excellent source of antioxidants. **Objective:** To evaluate the antimicrobial potential of copper nanoparticles (CuONPs) derived from *Moringa oleifera* pods against urinary tract-infecting microbes. **Methods:** Phyto constituents of the *Moringa oleifera* pod were screened. CuONPs were synthesized from *Moringa oleifera* pod, and it was characterized using UV-visible spectroscopy, FTIR, and SEM. Antioxidant activity of CuONPs was also determined. CuONPs discs at 50, 75, and 100 μ g/ml were prepared and tested for antimicrobial action against *Escherichia coli*, *Enterococcus faecalis*, *Klebsiella pneumonia*, *Streptococcus aureus*, and *Candida albicans*. The integrity of the *E.coli* was assayed by determining the lactate dehydrogenase activity. **Results:** GCMS analysis revealed the presence of Di-n-Octyl Phthalate and 2, 2-diethoxy Propane presence in the *Moringa oleifera* pod. Antioxidant assay revealed the free radical scavenging property of CuONPs. UV- VIS confirmed the synthesis of CuONPs by showing the λ Vmax at 220nm. SEM analysis revealed the CuONPs size in 40 to 160nm. The FTIR analysis exhibited the presence of OH and C = C groups in the CuONPs. The *klebsiella pneumoniae* was the most susceptible strain for CuONPs, followed by *Escherichia coli* and *Candida albicans*. *E. coli* showed a significant LDH activity at high concentration of CuONPs. **Conclusion:** The CuONPs synthesized from the *Moringa oleifera* pod exhibited significant antimicrobial activity against the microbes.

1. Introduction

Nanotechnology provided a scientifically sound method for generating nanostructures with improved functionality [1]. Any particle with a 1–100 nm range in size is called a nanoparticle (NPs) [2]. Being a Nano-size range

can afford a wide surface for the discovering of antimicrobial agent [3]. These Manipulative functionalities and wide applications sparked the scientific community to develop eco-friendly nanoparticles [4]. Eco-friendly NPs mean the green synthesis of NPs using bacteria,

Abbreviations: CuONPs, Copper nanoparticles; FTIR, Fourier Transform Infrared Spectroscopy; SEM, Scanning electron microscopy; LDH, Lactate dehydrogenase; GCMS, Gas Chromatography-Mass Spectrometry; NICM, National Collection of Industrial Microorganisms; NADH, nicotinamide adenine dinucleotide (NAD) + hydrogen; DPPH, 2,2-diphenyl-1-picrylhydrazyl; NBT, Nitro blue tetrazolium, KBr, Potassium bromide

*Corresponding author: sankar7950@gmail.com, Sankar.m@rajalakshmi.edu.in

doi: [10.61186/jmp.23.89.17](https://doi.org/10.61186/jmp.23.89.17)

Received 15 May 2024; Received in revised form 8 July 2024; Accepted 20 July 2024

© 2023. Open access. This article is distributed under the terms of the Creative Commons Attribution-NonCommercial 4.0 International License (<https://creativecommons.org/licenses/by-nc/4.0/>)

fungi, and plant extract rather than the deployment of conventional physical and chemical methods [5]. Numerous studies have been reported the use of plant extracts to synthesize metal-ion-based NPs with significant antimicrobial activity [6]. Basically, phytochemical constituents act as the reduced agent to synthesize green NPs [7]. *Moringa olifera* Lam, commonly called drumstick predominantly found in South Asia. The plant is highly valued because of its micronutrients used to treat various illnesses. Especially leaves have been reported as anticancer, cardioprotective, wound healing, hepatoprotective, and antimicrobial activities [8]. Moreover, *Moringa olifera* is considered the best resource for the rare combination of phytochemical constituents such as beta-sitosterol, caffeoylquinic acid, zeatin, quercetin, and kaempferol [9]. Virk *et al* 2023 recorded the rapid formation of NPs from *Moringa olifera* leaves [10]. Kalaiyan *et al* 2021 reported the significant antimicrobial action of the NPs from *Moringa olifera* leaves [11]. Recent studies have also shown the antimicrobial activity of silver nanoparticles synthesized from *Moringa olifera* [12]. Hence, the present study was focused on synthesizing the CuONPs using *Moringa oleifera* pod and evaluating the antimicrobial activity against the urinary tract infecting microbes.

2. Materials and methods

2.1. Chemicals

The chemicals and reagents used in the study were procured from the HI Media Laboratories.

2.2. Preparation of aqueous extract.

Moringa oleifera Pods were collected and washed with the distilled water. The cleaned pods were dried and grounded using distilled water. After grinding, the extract was filtered in

the Whatman filter paper. The filtrated extract was used to synthesize the copper nanoparticle.

2.3. *Moringa oleifera* pod GCMS Analysis

Phytochemical constituents present in *Moringa oleifera* pods were screened using a GCMS instrument (Shimadzu GC/MS-QP2010 Plus) equipped with a ZB-1 MS embedded silica column (30 m × 0.25 mm ID, 0.25 µm film thickness). The analysis was conducted in Electron Ionization mode (70 eV) with helium used as the mobile phase at a flow rate of 1 mL/min. The injection temperature was set at 250 °C. The column temperature started at 50 °C, held for 3 minutes, and then increased by 10 °C per minute up to 300 °C. The final temperature of 300 °C was maintained for 10 minutes. A 1.0 µL sample was injected in split mode. The relative percentages of each compound were recorded, and spectral configurations were obtained from the mass spectral database.

2.4. Synthesis of copper nanoparticle

Copper nanoparticles (CuONPs) were synthesized as per Pagar *et al.* (2020) [13]. Copper sulphate pentahydrate at 1mM, 2mM, 2.5mM, 3mM, and 3.5mM/mL was added to a clean 50 mL beaker containing 10 mL of an aqueous extract of *Moringa oleifera* pods. The mixture was stirred constantly on a magnetic stirrer at 500 rpm for 25 minutes. After a short while, the colourless solution turned dark brown. The resulting solution was centrifuged at 4000 rpm for 15 minutes at room temperature. The residue at the bottom of the centrifuge tube was collected and subjected to combustion in a muffle furnace at 400 °C for 1 hour. After combustion, a fine dark-coloured powder was obtained, stored, and used for various assays.

2.5. Determination of Antioxidant activity

2.5.1. DPPH scavenging activity assay

The antioxidant activity of CuONPs was assessed as per Ansar et al. (2020) [14]. CuONPs at concentrations of 50, 75, 100, and 125 $\mu\text{g}/\text{mL}$ were mixed with 0.1 mM DPPH and incubated at room temperature for 15 minutes. Absorbance was then measured at 517 nm, with methanol as a blank. The decrease in DPPH content indicates the scavenging activity of CuONPs, which was calculated as a percentage inhibition compared to vitamin C used as the standard.

DPPH scavenging activity = standard absorbance (standard absorbance – blank absorbance) / standard absorbance $\times 100$

2.5.2. Determination of Nitric oxide scavenging activity

The nitric oxide scavenging activity of CuONPs was determined following the method described by Patel Rajesh et al. (2011) [15]. Different concentrations of CuONPs were mixed with 2 mL of Fe-NPs and incubated at room temperature for 2 hours. Subsequently, 0.5 mL of the incubated mixture was combined with 1 mL of sulfanilic acid and left at room temperature for 5 minutes. To this reaction mixture, 0.1 % naphthyl ethylenediamine dihydrochloride was added and incubated again at room temperature for 30 minutes. The absorbance was then recorded at 546 nm. The nitric oxide scavenging activity of CuONPs was calculated and expressed as a percentage inhibition.

% scavenging activity = (T₀ (control) – T (test)) / T₀ $\times 100$

2.5.3. Determination of Superoxide anion scavenging activity

The superoxide anion scavenging activity of CuONPs was determined as per Nishikimi et al 1972 [16]. In brief, reaction mixture was

prepared by adding varying concentrations of CuONPs with 1 ml of 100 mM phosphate buffer (pH 7.4), 468 μM NADH, 156 μM NBT and 60 μM PMS. Then the reaction mixture was mixed well and incubated at room temperature for 5 mts. The amount of formazan complex is directly proportional to the scavenging activity, and it was detectable at 560nm.

2.5.4. Determination of Hydroxyl radical-scavenging activity of CuONPs

Hydroxyl radical-scavenging activity of the CuONPs was determined based on Smirnof et al. 1989 [17]. A reaction mixture was prepared by adding 1ml each of 9 mM ferrous sulphate, of 9 mM salicylic acid, and hydrogen peroxide with varying concentrations of 1ml of CuONPs and incubated in a boiling water bath for 1 hr at 37 °C. After the incubation reaction, the mixture was cooled and read at 510nm. The Hydroxyl radical-scavenging activity of the CuONPs was calculated and expressed in percentage.

2.6. Characterization of copper nanoparticles synthesized from the *Moringa oleifera*

2.6.1. UV-Visible spectroscopic analysis

The CuONPs synthesized using the *Moringa oleifera* were subjected to the UV Visible spectrophotometer (Shimadzu1700, Double beam, Japan). The reduction of copper nanoparticles was continuously monitored in the UV- spectrophotometer at 220-700nm [18].

2.6.2. FTIR analysis for the nanoparticles

The FTIR spectrum of the CuONPs was recorded based on the KBr Disc method. The dried CuONPs were ground in the presence of anhydrous KBr and compressed and formulated as a pellet. The pellet was scanned in the FTIR spectra in 4000-400 cm^{-1} [18].

2.6.3. Scanning electron microscopic (SEM) analysis

The surface morphology dimension and the size of the CuONPs were visualized in the SEM (ZEISS Supra 40, Germany) under the standard atmospheric condition. The samples were placed on the glass slide and spread evenly and magnified [18].

2.7. Microorganisms

The following strains, *Escherichia coli* (NICM 2065), *Enterococcus faecalis* (NICM 5021), *Klebsiella pneumonia*, *Streptococcus aureus* (NICM 5021), and *Candida albicans* were procured from the national chemical laboratory.

2.7.1. Antibacterial sensitivity assay

The antibacterial activity of CuONPs was determined according to Kim et al. (1995) [19]. Mueller-Hinton agar plates were swabbed with an overnight culture. Filter paper disks were prepared by soaking them in CuONPs solutions of three different concentrations: 50 $\mu\text{g}/\text{mL}$, 75 $\mu\text{g}/\text{mL}$, and 100 $\mu\text{g}/\text{mL}$, until saturated. The soaked paper disks were then placed on the inoculated Mueller-Hinton agar plates. A standard ampicillin 20 μg disk was used as a positive control. All plates were incubated at $37 \pm 2^\circ\text{C}$ for 24 hours. After incubation, the diameter of the inhibition zone was measured in millimeters using a vernier caliper.

2.7.2. Antifungal assay

The antifungal assay was conducted according to Bauer et al. (1996) [20]. The fungal strain inoculum was spread over a potato dextrose agar medium. Paper disks containing different concentrations of CuONPs (50 $\mu\text{g}/\text{mL}$, 75 $\mu\text{g}/\text{mL}$, and 100 $\mu\text{g}/\text{mL}$) were placed on the surface of the medium. The plates were then incubated at $37 \pm 2^\circ\text{C}$ for 24 hours in triplicates. The antifungal activity of CuONPs was determined by measuring the diameter of the zone of inhibition in millimeters.

2.8. Assay of Lactate dehydrogenase activity

The protein leakage from *E. coli* was detected by assaying LDH activity. The LDH assay was performed according to Kalińska et al. (2019) [21], with slight modifications. Bacterial cells (5×10^3 cells/well) were incubated in 96-well plates containing the medium and 50, 75, 100, and 125 $\mu\text{g}/\text{mL}$ of CuONPs for 24 hours. For the control, *E. coli* was incubated in plates without CuONPs. After incubation, the plates were centrifuged, and 50 μL of the supernatant was transferred to new 96-well plates. Then, LDH working solutions were added to each well, and the absorbance was measured at 490 nm. LDH activity was expressed as nmole/min/mL of pyruvate liberated.

2.9. Statistical analysis

The inhibition diameters (mm) zone is represented in mean \pm SD, where $N = 3$. The mean \pm SD inhibition zone diameters of the CuONPs and the standard control (ampicillin) were analyzed in the one-way ANOVA variance and followed by Turkey –Kramer multiple comparisons were carried out using Graph pad prism. The P values ≤ 0.05 are considered significant when comparing one strain with another.

3. Results

3.1. GCMS analysis of *Moringa oleifera* pod.

Figure 1 depicts the characteristic absorption spectra of *Moringa oleifera* pod on GCMS analysis. A total of 51 phytochemicals were present in the *Moringa oleifera* pod. Among Dinit-Octyl Phthalate, 2,2-diethoxy Propane, and Piperidine, 1-5-1,3-benzodioxol occupied the major proportion. The area occupied by the respective phytochemicals and their retention times are shown in Tables 1 and 2.

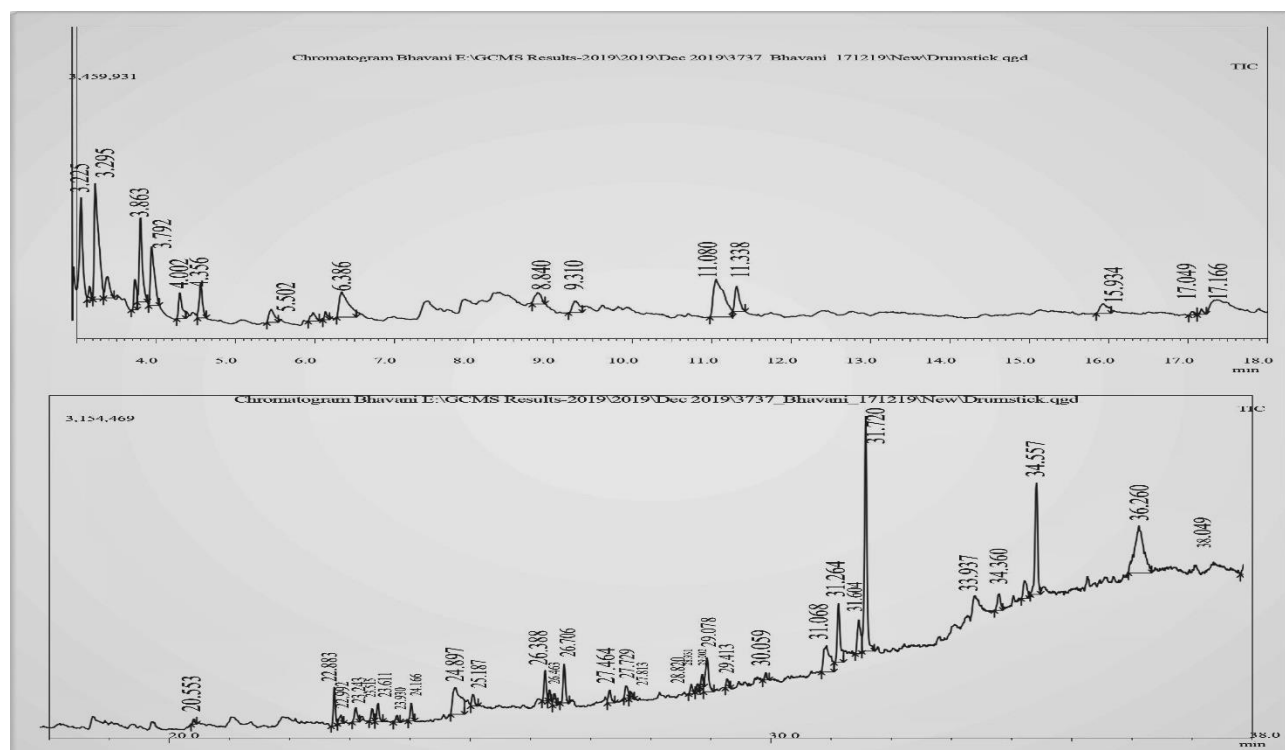


Fig. 1. The Chromatogram and the mass spectrometric profile of *Moringa oleifera* pod on GCMS analysis

Table 1. The phytochemical constituents in the *Moringa oleifera* pod on GCMS analysis

Peaks	Retention Time (mts)	Area %	Name of the compound
1	3.225	0.52	1.99 2,5-Furandione, 3,4-dimethyl
2	3.295	8.44	3.79 2,2-diethoxy Propane
3	3.448	1.65	3.99 2-Propyn-1-OL
4	3.792	1.43	2.45 l-Alanine, N-methoxycarbonyl- methyl ester
5	3.863	4.48	2.76 1-hexen-3-OL
6	4.002	3.98	3.51 1-Propanol, 2,2-dimethyl-, acetate
7	4.356	1.63	3.25 1-Butanamine, n-Butylidene
8	4.617	1.85	2.72 2-pentanone, 4-hydroxy-4-methyl
9	5.502	1.26	4.95 3,4-hexanedione, 2,2,5,5-tetrameth
10	6.027	0.69	4.23 2H-Pyran, tetrahydro
11	6.182	0.41	2.62 2-Butyl-(2-methylbutylidene)-AM
12	6.386	3.98	8.11 2(3H)-Furanone, 5-Methyl
13	8.840	1.26	5.66 6-Dodecanone
14	9.310	1.36	6.04 2,5-Anhydro-1,6-Dideoxyhexo-3,4-D
15	11.080	6.81	9.36 1,5-Anhydro-6-Deoxyhexo-2,3-dilouse
16	11.338	1.94	4.03 Pentanedioic acid, Ethyl Methyl Ester
17	15.934	1.35	7.02 Cyclohexane, 1,2,3-Trimethoxy-, S
18	17.049	0.19	2.80 Tetradecone, 1-Chloro
19	17.166	0.26	2.36 Cyclododecane
20	20.553	0.23	2.77 E-11,13-Tetradecadien-1-ol

Table 1. The phytochemical constituents in the *Moringa oleifera* pod on GCMS analysis (Continued)

Peaks	Retention Time (mts)	Area %	Name of the compound
21	22.883	1.41	2.29 Neophytadiene
22	22.992	0.44	3.27 2-Pentadecanone, 6,10,14-Trimethyl
23	23.243	0.81	3.45 (8Z)-14-Methyl-8-Hexadecen-1-OL
24	23.515	0.48	2.45 3,7,11,15-Tetramethyl-2-Hexadecen-1-ol
25	23.611	0.81	2.80 1-Hexadecanol

Table 2. The phytochemical constituents in the *Moringa oleifera* pod on GCMS analysis

Peaks	Retention Time (mts)	Area %	Name of the compound
26	23.930	0.31	2.75 N,N-Bimethyl-3-Buten-1-Amine
27	24.166	0.75	2.61 Pentadecanoic acid, 14-Methyl-, Methyl Ester
28	24.897	3.98	9.24 9-Octadecenoic acid (Z)
29	25.187	0.55	2.97 Hexadecanoic acid, 2-Oxo-, Methyl ester
30	26.388	1.29	2.64 3-Eicosene
31	26.463	0.39	2.11 9,12-Octadecadienoic acid, Methyl Ester, (E,E)
32	26.541	0.50	2.72 9-Octadecenoic acid (Z)-, Methyl E
33	26.706	1.73	2.78 2-Hexadecen-1-OL, 3,7,11,15-Tetrame
34	27.464	0.67	3.26 2-Ethylhexyl (2E)-3- 4-Methoxyphenyl
35	27.729	0.73	3.82 Dodecanamide
36	27.813	0.36	3.16 Heptyltriacetyl ether
37	28.820	0.44	2.86 Carbamic acid, 2-(Dimethylamino) Ethyl ester
38	28.931	0.36	2.68 Dioctadecylphosphonate
39	29.002	0.54	2.65 3-Methyl-2-Octanol
40	29.078	2.18	4.03 12-O-acetylengol 8-tiglate
41	29.413	0.42	2.81 2-Ethylhexyl (2e)-3-4-methoxyphenyl
42	30.059	0.27	2.22 Hexanedioic acid, Dioctyl ester
43	31.068	3.22	7.60 2-Methyl-Z,Z-3,13-Octadecadienol
44	31.264	3.35	3.55 Trichloroacetic acid, Pentadecyl ester
45	31.604	2.07	3.83 hexadecanoic acid 2-hydroxy-1- (hydroxymethyl)ethyl ester
46	31.720	10.69	2.84 Di-n-Octyl Phthalate
47	33.937	1.02	3.79 1,3-Benzenedicarboxylic acid, bis 2-ethylhexyl ester
48	34.360	1.25	4.37 Piperidine, 1-5-1,3-benzodioxol
49	34.557	5.22	2.93 Squalene
50	36.260	7.95	10.53 Piperidine, 1-5-1,3-benzodioxol
51	38.049	2.09	5.33 Ethyl Iso-Allocholate

3.2. Copper nanoparticle synthesis

The synthesis of copper nanoparticles was confirmed by visualizing the appearance of a reddish-brown colour from a colorless solution at 3 mM of copper sulphate. Whereas, at 1 mM, 2 mM, 2.5 mM, and 3.5 mM of copper sulphate

there is no specific colour change inferred in the solution. Hence, the optimum concentration of copper sulphate is 3 mM for copper nanoparticle synthesis.

3.3. Antioxidant activity of copper nanoparticles

The free radical scavenging activity of copper nanoparticles was screened; the results obtained are depicted in figure 2. 83 % DPPH free radicals were scavenged at 125 $\mu\text{g}/\text{ml}$ of copper nanoparticles. Whereas, in the presence of 50, 75, and 100 $\mu\text{g}/\text{ml}$ copper nanoparticles scavenge 60 %, 64 %, and 70 % DPPH of free radicals. Copper nanoparticles at 125 $\mu\text{g}/\text{ml}$ scavenge 83 % of superoxide anion, whereas at 50, 75, and 100 $\mu\text{g}/\text{ml}$ scavenge 59 %, 64 %,

and 78 %, respectively. Copper nanoparticles at 125 and 100 $\mu\text{g}/\text{ml}$ scavenge 80 % of the nitric oxides. But at 50 and 75 $\mu\text{g}/\text{ml}$, copper nanoparticles scavenged 65 % and 70 % of nitric oxide radicals. The hydroxyl ions scavenging activity of copper nanoparticles was also analyzed. At 125 $\mu\text{g}/\text{ml}$, copper nanoparticles scavenged 83% of hydroxyl ions. But at 50, 75, and 100 $\mu\text{g}/\text{ml}$, copper nanoparticles scavenged 63 %. 69 % and 73 % of hydroxyl ions.

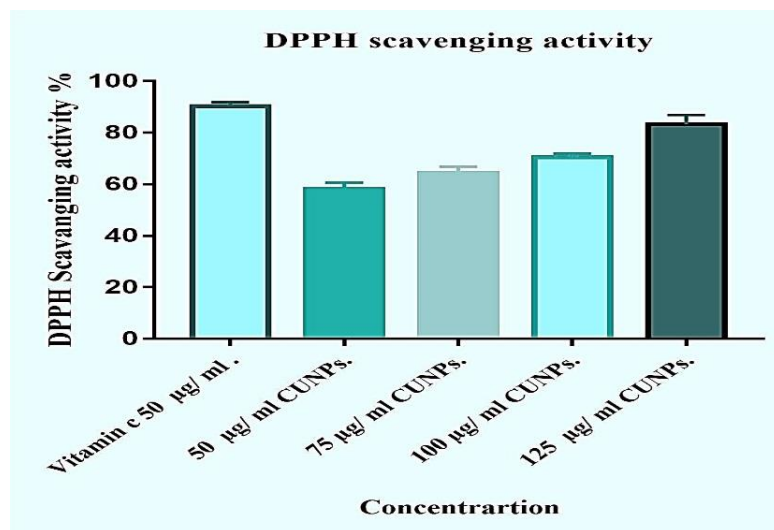


Fig. 2. (A) DPPH scavenging activity of copper nanoparticles

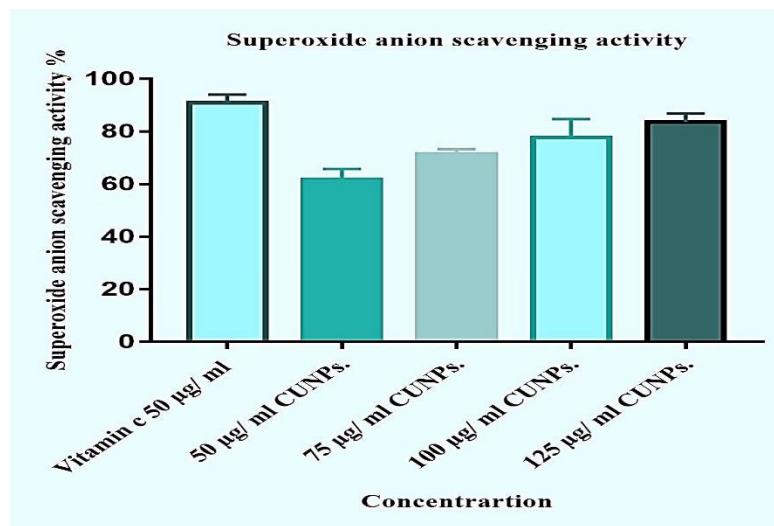


Fig. 2. (B) Superoxide anion scavenging activity of copper nanoparticles

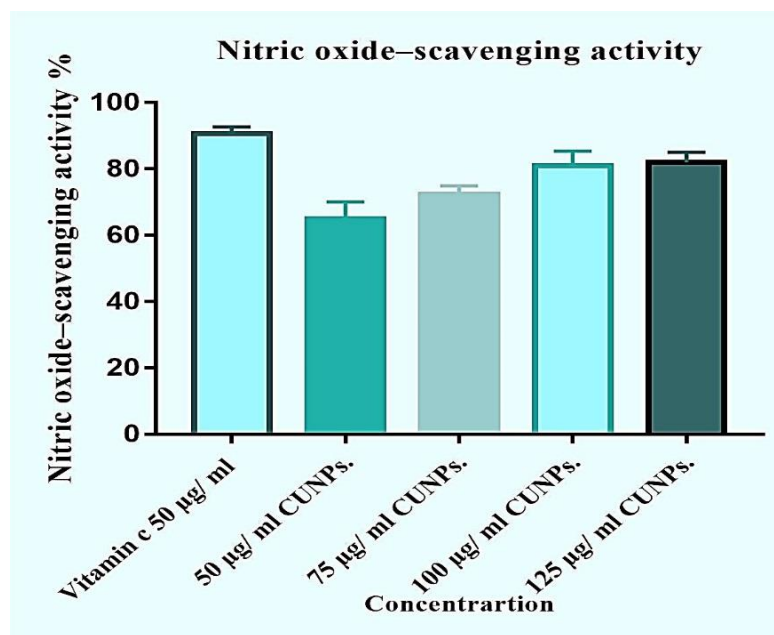


Fig. 2. (C) Nitric oxide scavenging activity of copper nanoparticles

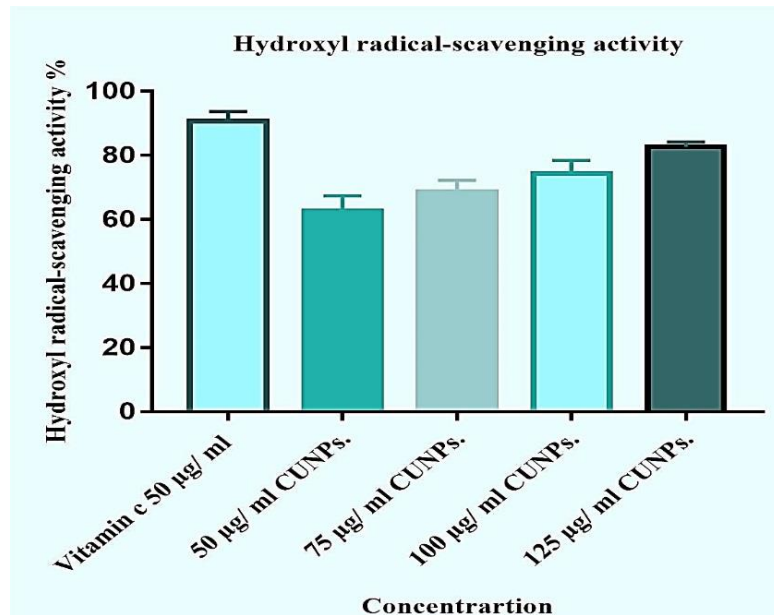


Fig. 2. D Hydroxyl radical scavenging activity of copper nanoparticles

3.4. UV-Visible spectroscopic analysis of copper nanoparticles synthesized from the *Moringa oleifera* pod.

Figure 3 depicts the λ Vmax of copper nanoparticles. At 220 nm, copper nanoparticles showed the maximum absorption. Hence, the

absorption spectra of the copper nanoparticle are found to be 220 nm.

3.5. SEM analysis of copper nanoparticles

The size and surface morphology of the copper nanoparticles were studied using the SEM. Figure 4 depicts the surface morphology

of copper nanocrystals analyzed by the SEM. Spherical and tubular-shaped copper nanocrystals were observed in aggregates, and each nanocrystal ranged in between 40.1 and 180.3 nm.

3.6. FTIR spectra of copper nanoparticles

The FTIR spectra of copper nanoparticles are shown in Figure 5. The broad peak at 3300 cm^{-1} and the sharp peak at 1635.64 cm^{-1} correspond to the OH and C=C stretch, respectively.

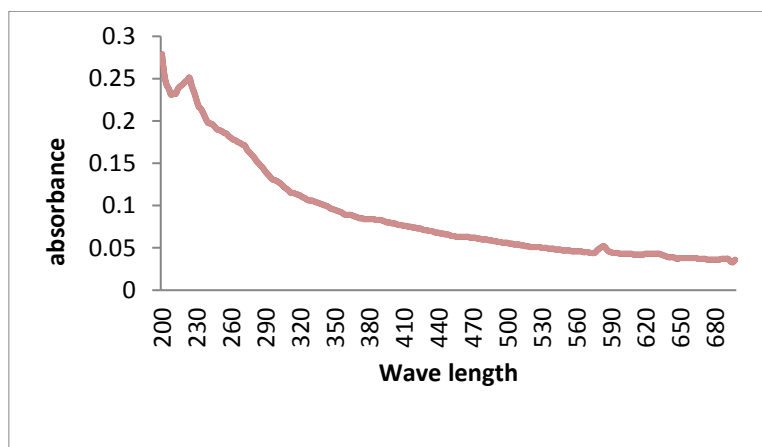


Fig. 3. The UV-Visible spectroscopy analysis of the copper nanoparticles

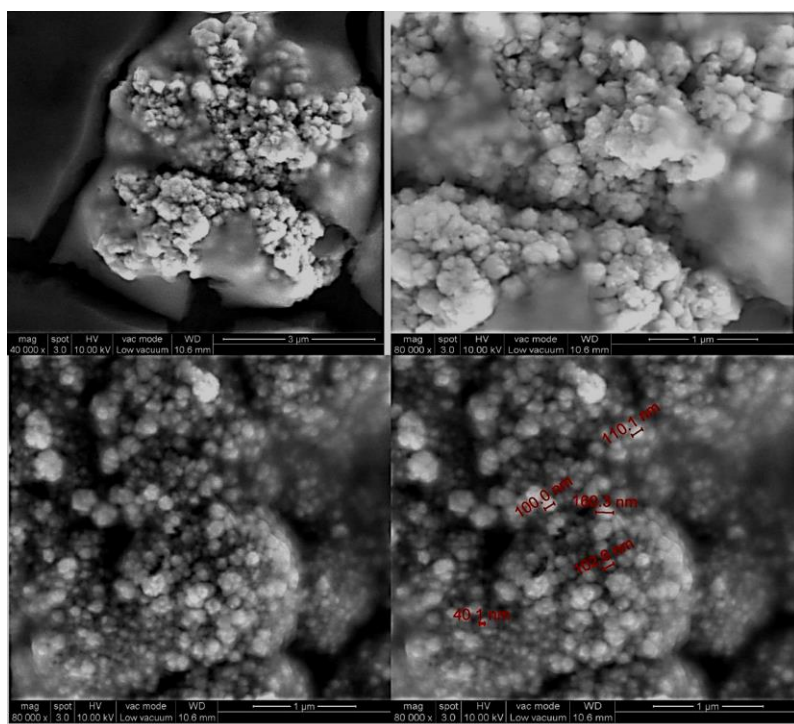


Fig. 4. SEM images of copper nanoparticles synthesized from the *Moringa oleifera* pod. The Spherical and tubular copper nanoparticles in aggregates range from 40.1 to 110.3nm on SEM analysis.

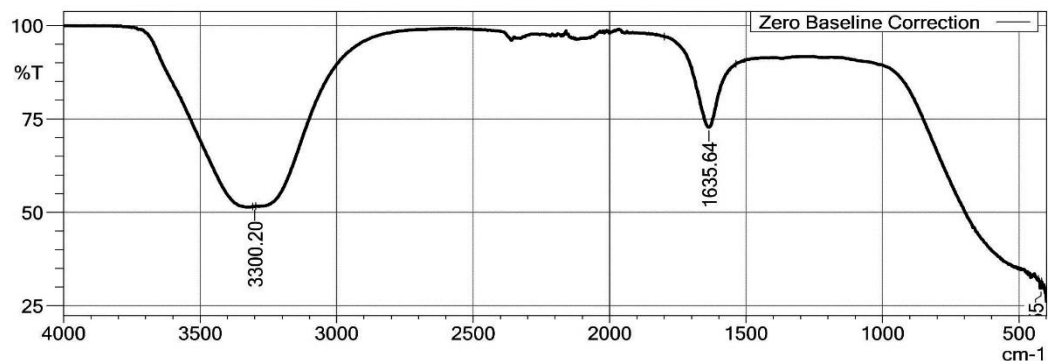


Fig. 5. The FTIR spectra of the copper nanoparticles
FTIR spectra for the CuONPs. The broadband at 3300 cm⁻¹ and a sharp band at 1635.64 cm⁻¹ correspond to OH and C = C vibration stretches.

3.7. The Antimicrobial activity of copper nanoparticles

The antimicrobial activity of copper nanoparticles was studied, and the results obtained are depicted in table 3 and figure 4. Figure 6 depicts the antimicrobial activity of copper nanoparticles. The *Klebsiella pneumoniae* was found to be most sensitive among given species to the copper nanoparticles. Followed by *E. coli*, *C. albicans*,

Enterococcus faecalis, and *Streptococcus aureus* were considered to be least susceptible for the copper nanoparticles. However, all the species were susceptible at a high concentration (100 µg/mL) of copper nanoparticles. The *Escherichia coli*, *Enterococcus faecalis*, *Klebsiella pneumoniae*, *Streptococcus aureus*, and *Candida albicans* scored the least susceptibility at 50 µg/mL and 75 µg/mL of copper nanoparticles.

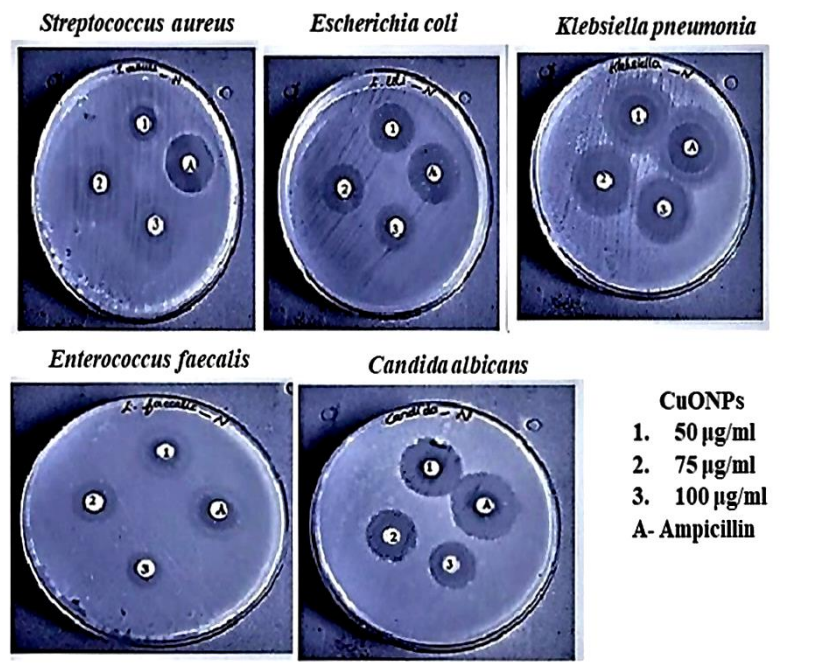


Fig. 6. The antimicrobial activity of the Copper nanoparticles

Table 3. The antimicrobial action of copper nanoparticles

Test Organisms	50 $\mu\text{g/ml}$ CuONPs	75 $\mu\text{g/ml}$ CuONPs	100 $\mu\text{g/ml}$ CuONPs	20 $\mu\text{g/ml}$ Amp
<i>E. coli</i>	6.1 \pm 0.9 ^{bc}	7.2 \pm 0.8 ^c	9 \pm 1.0	11.6 \pm 1 ^c
<i>Klebsilla pneumonia</i>	9.4 \pm 0.7 ^{acd}	10.4 \pm 1.2 ^{abd}	11.2 \pm 0.7 ^{abc}	12.8 \pm 0.8 ^{ac}
<i>Enterococcus faecalis</i>	4.2 \pm 0.8	7.2 \pm 1 ^c	8.1 \pm 1.1	10.2 \pm 1.1
<i>Staphylococcus aureus</i>	4.3 \pm 0.7	5.4 \pm 0.7	8.0 \pm 1.3	10.1 \pm 1
<i>Candida albicans</i>	5.9 \pm 0.8 ^{bc}	8.2 \pm 0.9 ^{abc}	11.2 \pm 1 ^{abc}	12.3 \pm 0.9 ^c

Values are expressed as mean \pm SD of zone of inhibition in diameter (mm). The superscript ^a is $p \leq 0.05$ significant different in between *E. coli* vs other strains. The superscript ^b is $p \leq 0.05$ significant different in between *E. faecalis* vs other strains. The superscript ^c is $P \leq 0.05$ significant different in between *S. aureus* with other strains and superscript ^d significant different in between *C. albicans* with others.

3.8. *E. coli* integrity assay

LDH activity in culture medium was assayed to ascertain the integrity of the *E. coli* in the presence of copper nanoparticles. Figure 7 represents the LDH activity of the *E. coli* in the medium. At 100 and 125 $\mu\text{g/ml}$ of copper

nanoparticle treatment, *E. coli* displayed significant activity in the medium when compared to the control. At the same time, a non-significant LDH activity was inferred at 50 and 75 $\mu\text{g/ml}$ of copper nanoparticle treatment.

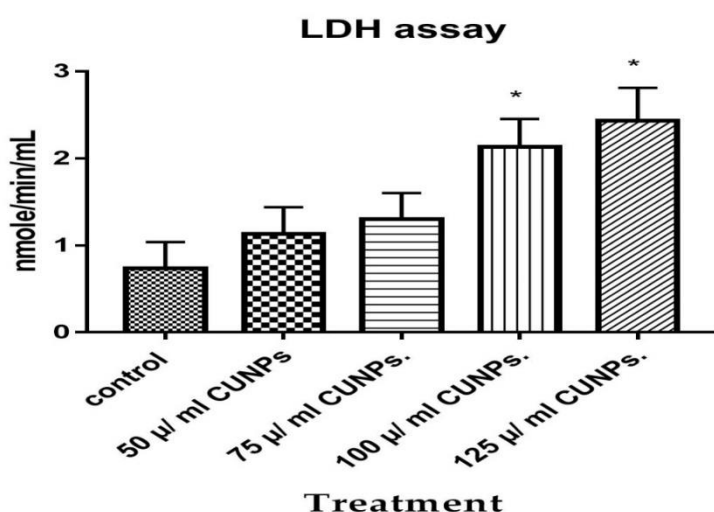


Fig. 7. Impact of copper nanoparticle on *E. coli* membrane integrity.

$N = 3$, values are expressed as in the form of mean \pm SD, $P \leq 0.05^*$ considered significant compared to 50 $\mu\text{l/ml}$ CUNPs.

4. Discussion

Over the years, traditional antibiotics used to treat bacterial infections have been developed, but multidrug-resistant strains (MDR) have become a significant concern. Therefore, it is crucial to seek alternatives to combat these MDR strains and their associated complications [22]. In recent years, nano-based antimicrobial

agents have garnered attention and are considered alternative approaches to controlling pathogenic strains with minimal risk. [23]. Therefore, the study aimed to synthesize CuONPs using *Moringa oleifera* pods and evaluate their antimicrobial potential against urinary tract infection-causing microbes. CuONPs were synthesized using copper

sulphate as the precursor and *Moringa oleifera* pods as the capping agent. The colourless solution changed to reddish-brown, indicating successful synthesis of CuONPs, which was confirmed by UV-visible spectroscopy. A strong absorbance peak at 220 nm confirmed the presence of copper nanoparticles and marking the λ Vmax. The reddish-brown colour change and the characteristic absorbance at 220 nm are attributed to surface plasmon resonance and serving as signatures of copper nanoparticle synthesis [24]. FTIR is used to examine the functional groups in given particles [25]. In the current investigation, the FTIR spectrum of CuONPs shows two peaks: a broad peak at 3300 cm^{-1} and a sharp peak at 1635.64 cm^{-1} . The broad peak at 3300 cm^{-1} is related to OH stretching, while the sharp peak at 1635.64 cm^{-1} corresponds to C = C stretching [26, 27]. The OH stretching is attributed to phenolic compounds such as flavonoids, alkaloids, and terpenoids present in *Moringa oleifera*, which may act as capping agents for the synthesis of CuONPs [28]. Previous studies have also indicated that C = C stretching is involved in the formation of CuONPs from *Moringa oleifera* [29].

SEM analysis is widely employed to reveal the surface morphology and size of nanostructures [30]. In the present study, a tubular and spherical-shaped copper nano crystal was observed in aggregates and each nanocrystal ranges from 40 to 110 nm. Our findings are in correlation with the report of Andualem et al. (2020) [31]. The aggregation of copper nanocrystals is attributed to the presence of secondary metabolites in *Moringa oleifera* and is also influenced by the polarity and electrostatic attraction of copper nanocrystals with salt precursors [32].

The antimicrobial assay indicated that *K. pneumoniae* was the most susceptible to the

copper nanoparticles, followed by *E. coli*, *S. aureus*, and *C. albicans*. Particularly, at high concentrations of CuONPs, all organisms displayed growth inhibition. Notably, gram-negative bacteria such as *K. pneumoniae* and *E. coli* exhibited the maximum susceptibility to CuONPs compared to the gram-positive strains such as *E. faecalis* and *S. aureus*. The difference in susceptibility between the gram-positive and gram-negative bacterial strains to CuONPs observed in our current finding is highly correlating with earlier reports [33]. The variation in the susceptibility of bacterial strains to CuONPs is attributed to opposite charges and electrostatic interactions. Additionally, since the peptidoglycan layer of bacteria is negatively charged, differences in the binding of Cu^{2+} ions to the bacterial cell wall may cause variations in susceptibility. Another reason for the susceptibility differences is that Gram-negative bacterial strains allow more copper ions to reach the plasma membrane compared to Gram-positive bacteria [33]. In the current observation, fungicidal activity against *C. albicans* was also noted at certain concentrations of CuONPs. The fungicidal effect of the CuONPs might be due to disturbances in the replication and transpiration of the fungi [34]. The LDH assay indicates the status of cellular integrity. In the current observation, higher LDH activity was detected in the medium of *E. coli* incubated with CuONPs. The increased LDH activity may be the result of leakage from bacterial cells due to oxidative stress resultant damage in the cell wall of bacteria [35].

5. Conclusion

The copper nanoparticles synthesized from the *Moringa oleifera* pod displayed significant antimicrobial activity against infecting urinary tract microbes.

Author contribution

B. S. carried out the entire work under the supervision of M. S.

Conflicts of interest

There is no conflict of interest.

References

1. Payal and Pandey P. Role of nanotechnology in electronics: A review of recent developments and patents. *Recent Pat. Nanotechnol.* 2022; 16(1): 45-66. doi: 10.2174/1872210515666210120114504.
2. Joudeh N and Linke D. Nanoparticle classification, physicochemical properties, characterization, and applications: a comprehensive review for biologists. *J. Nanobiotechnol.* 2022; 20: 262. doi: 10.1186/s12951-022-01477-8.
3. Mondal SK, Chakraborty S, Manna S and Mandal SM. Antimicrobial nanoparticles: current landscape and future challenges. *RSC Pharmaceutics.* 2024. doi: 10.1039/D4PM00032C.
4. Abuzeid HM, Julien CM, Zhu L and Hashem AM. Green synthesis of nanoparticles and their energy storage, environmental, and biomedical applications. *Crystals* 2023; 13(11): 1576. doi: 10.3390/crust13111576.
5. Mayegowda SB, Sarma G, Gadilingappa MN, Alghamdi S, Aslam A, Refaat B, Almehmadi M, Allahyani M, Alsaiari AA, Aljuaid A and Al-Moraya IS. Green-synthesized nanoparticles and their therapeutic applications: A review. *Green Processing and Synthesis.* 2023; 12: 1-17. 20230001. doi: 10.1515/gps-2023-0001.
6. Susanti D, Haris MS, Taher M and Khotib J. Natural products-based metallic nanoparticles as antimicrobial agents. *Front. Pharmacol.* 2022; 13: 895616. doi: 10.3389/fphar.2022.895616.
7. Pradeep M, Kruszka D, Kachlicki P, Mondal D and Franklin G. Uncovering the phytochemical basis and the mechanism of plant extract-mediated eco-friendly synthesis of silver nanoparticles using ultra-performance liquid chromatography coupled with a photodiode array and high-resolution mass spectrometry. *ACS Sustainable Chemistry & Engineering.* 2021; 10(1): 562-71. doi: 10.1021/acssuschemeng.1c06960.
8. Kashyap P, Kumar S, Riar CS, Jindal N, Baniwal P, Guiné RP, Correia PM, Mehra R and Kumar H. Recent advances in Drumstick (*Moringa oleifera*) leaves bioactive compounds: Composition, health benefits, bioaccessibility, and dietary applications. *Antioxidants.* 2022; 11(2): 402. doi: 10.3390/antiox11020402.
9. Pop OL, Kerezsi AD and Ciont C. A comprehensive review of *Moringa oleifera* bioactive compounds—cytotoxicity evaluation and their encapsulation. *Foods* 2022; 11(23): 3787. doi: 10.3390/foods11233787.
10. Virk P, Awad MA, Alsaif SS, Hendi AA, Elobeid M, Ortashi K, Qindeel R, El-Khadragy MF, Yehia HM, El-Din MF and Salama HA. Green synthesis of *Moringa oleifera* leaf nanoparticles and an assessment of their therapeutic potential. *Journal of King Saud University-Science.* 2023; 35(3): 102576. doi: 10.1016/j.jksus.2023.102576.
11. Kalaiyan G, Suresh S, Prabu KM, Thambidurai S, Kandasamy M, Pugazhenthiran N, Kumar SK and Muneeswaran T. Bactericidal activity of *Moringa oleifera* leaf extract assisted green synthesis of hierarchical copper oxide microspheres against pathogenic bacterial

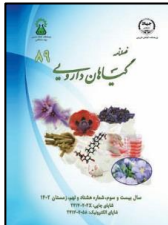
Acknowledgment

The authors thank the Rajalakshmi Engineering College for providing the support to carry out the work.

- strains. *Journal of Environmental Chemical Engineering*. 2021; 9(1): 104847. doi: 10.1016/j.jece.2020.104847.
- 12.** Haris Z and Ahmad I. Green synthesis of silver nanoparticles using *Moringa oleifera* and its efficacy against gram-negative bacteria targeting quorum sensing and biofilms. *Journal of Umm Al-Qura University for Applied Sciences*. 2024; 10(1): 156-67. doi: 10.1007/s43994-023-00089-8.
- 13.** Pagar K, Ghotekar S, Pagar T, Nikam A, Pansambal S, Oza R, Sanap D and Dabhane H. Antifungal activity of biosynthesized CuO nanoparticles using leaves extract of *Moringa oleifera* and their structural characterizations. *Asian Journal of Nanoscience and Materials*. 2020; 3(1): 15-23. doi: 10.26655/AJNANOMAT.2020.1.2.
- 14.** Ansar S, Tabassum H, Aladwan NS, Naiman Ali M, Almaarik B, AlMahrouqi S, Abudawood M, Banu N and Alsubki R. Eco friendly silver nanoparticles synthesis by *Brassica oleracea* and its antibacterial, anticancer and antioxidant properties. *Scientific Reports*. 2020; 10(1): 18564. doi: 10.1038/s41598-020-74371-8.
- 15.** Patel Rajesh M and Patel Natvar J. In vitro antioxidant activity of coumarin compounds by DPPH, Super oxide and nitric oxide free radical scavenging methods. *Journal of Advanced Pharmacy Education & Research*. 2011; 1(1): 52-68.
- 16.** Nishikimi M, Rao NA and Yagi K. The occurrence of superoxide anion in the reaction of reduced phenazine methosulfate and molecular oxygen. *Biochemical and Biophysical Research Communications*. 1972; 46(2): 849-54. doi: 10.1016/s0006-291x(72)80218-3.
- 17.** Smirnoff N and Cumbes QJ. Hydroxyl radical scavenging activity of compatible solutes. *Phytochem*. 1989; 28(4): 1057-60. doi: 10.1016/0031-9422(89)80182-7.
- 18.** Srivastava AK and Dwivedi KN. Formulation and characterization of copper nanoparticles using *Nerium odorum* Soland leaf extract and its antimicrobial activity. *International Journal of Drug Development and Research*. 2018; 10: 29-34.
- 19.** Kim J, Marshall MR and Wei CI. Antibacterial activity of some essential oil components against five foodborne pathogens. *Journal of Agricultural and Food Chemistry*. 1995; 43(11): 2839-45. doi: 10.1021/jf00059a013.
- 20.** Bauer AW, Kirby WM, Sherris JC and Turck M. Antibiotic susceptibility testing by a standardized single disk method. *American Journal of Clinical Pathol*. 1966; 45(4_ts): 493-6. pubmed.ncbi.nlm.nih.gov/5325707/.
- 21.** Kalińska A, Jaworski S, Wierzbicki M and Gołębiewski M. Silver and copper nanoparticles—an alternative in future mastitis treatment and prevention?. *Int. J. Mol. Sci.* 2019; 20(7): 1672. doi: 10.3390/ijms20071672.
- 22.** Uddin TM, Chakraborty AJ, Khusro A, Zidan BRM, Mitra S, Emran TB, Dhamma K, Ripon MKH, Gajdács M, Sahibzada MUK, Hossain MJ and Koirala N. Antibiotic resistance in microbes: History, mechanisms, therapeutic strategies and future prospects. *Journal of Infection and Public Health*. 2021; 14(12): 1750-66. doi: 10.1016/j.jiph.2021.10.020.
- 23.** Nishshankage K, Fernandez AB, Pallewatta S, Buddhini PKC and Vithanage M. Current trends in antimicrobial activities of carbon nanostructures: potentiality and status of nanobiochar in comparison to carbon dots. *Biochar*. 2024; 6(1): 2. doi: 10.1007/s42773-023-00282-2.
- 24.** Fentie M, Chouhan G, Moges M and Tyagi P. Green synthesis of copper oxide nanoparticles using *Bryophyllum pinnatum* Leaf extract and

- its antibacterial potential against *Listeria monocytogenes*. *IJHS*. 2022; 6(S2): 5349-67. doi: 10.53730/ijhs.v6nS2.6345.
- 25.** Enders AA, North NM, Fensore CM, Velez-Alvarez J and Allen HC. Functional group identification for FTIR spectra using image-based machine learning models. *Analytical Chem.* 2021; 93(28): 9711-8. doi: 10.1021/acs.analchem.1c00867.
- 26.** Nzilu DM, Madivoli ES, Makhanu DS, Wanakai SI, Kiprono GK and Kareru PG. Green synthesis of copper oxide nanoparticles and its efficiency in degradation of rifampicin antibiotic. *Scientific Reports*. 2023; 13(1): 14030. doi: 10.1038/s41598-023-41119-z.
- 27.** Nandiyanto ABD, Ragadhita R and Fiandini M. Interpretation of Fourier transform infrared spectra (FTIR): A practical approach in the polymer/plastic thermal decomposition. *IJOST*. 2023; 8(1): 113-26. doi: 10.17509/ijost.v8i1.53297.
- 28.** Preethi DRA and Philominal A. Green synthesis of pure and silver doped copper oxide nanoparticles using *Moringa oleifera* leaf extract. *Materials Letters: X*. 2022; 13: 100122. doi: 10.1016/j.mlblux.2022.100122.
- 29.** Anas Ahzaruddin AT, Nik Nasihah NR, Adam SH, Mutalib MA, Mokhtar MH and Tang SG. Phytofabrication of Selenium nanoparticles with *Moringa oleifera* (MO-SeNPs) and exploring its antioxidant and antidiabetic potential. *Molecules* 2023, 28(14): 5322. doi: 10.3390/molecules28145322.
- 30.** Asano N, Lu J, Asahina S and Takami S. Direct observation techniques using scanning electron microscope for hydrothermally synthesized nanocrystals and nanoclusters. *Nanomaterials*. 2021; 11(4): 908. doi: 10.3390/nano11040908.
- 31.** Andualem WW, Sabir FK, Mohammed ET, Belay HH and Gonfa BA. Synthesis of Copper oxide nanoparticles using plant leaf extract of *Catha edulis* and its antibacterial activity. *J. Nanotechnol.* 2020; 2020(1): 2932434. doi: 10.1155/2020/2932434.
- 32.** Shi YE, Ma J, Feng A, Wang Z and Rogach AL. Aggregation-induced emission of copper nanoclusters. *Aggregate*. 2021; 2(6): e112. doi: 10.1002/agt2.112.
- 33.** Jabeen A, Khan A, Ahmad P, Khalid A, Wizrah MSI, Anjum Z, Alotibi S, Aloufi BH, Alanazi AM, Jefri OA and Ismail MA. Biogenic synthesis of levofloxacin-loaded copper oxide nanoparticles using *Cymbopogon citratus*: A green approach for effective antibacterial applications. *Heliyon*. 2024; 10(6): e27018. doi: 10.1016/j.heliyon.2024.e27018.
- 34.** Kamel SM, Elgobashy SF, Omara RI, Derbalah AS, Abdelfatah M, El-Shaer A, Al-Askar AA, Abdelkhalek A, Abd-Elsalam KA, Essa T and Kamran M. Antifungal activity of copper oxide nanoparticles against root rot disease in cucumber. *Journal of Fungi*. 2022; 8(9): 911. doi: 10.3390/jof8090911.
- 35.** Kim SH, Lee HS, Ryu DS, Choi SJ and Lee DS. Antibacterial activity of silver-nanoparticles against *Staphylococcus aureus* and *Escherichia coli*. *Microbiol. Biotechnol. Lett.* 2011; 39(1): 77-85.

How to cite this article: Sundar B, Madhavan S. Evaluation of antioxidant and antimicrobial action of copper nanoparticles synthesized from *Moringa oleifera* pods. *Journal of Medicinal Plants* 2024; 23(89): 17-31. doi: [10.61186/jmp.23.89.17](https://doi.org/10.61186/jmp.23.89.17)



ارزیابی اثر آنتیاکسیدانی و ضد میکروبی نانوذرات مس سنتز شده از غلاف مورینگا اولیفرا باوانی سوندار، سانکار مدهاوان*

گروه بیوتکنولوژی، کالج مهندسی راجالاکشمی، تاندalam، چنای، هندوستان

اطلاعات مقاله	چکیده
<p>مقدمه: یک گیاه دارویی سنتی جنوب هند و منبع عالی آنتی اکسیدان است. هدف: ارزیابی پتانسیل ضد میکروبی نانوذرات مس (CuONPs) مشتق شده از غلافهای <i>Moringa oleifera</i> در برابر میکروب‌های آلووده کننده دستگاه ادراری. روش بررسی: ترکیبات موجود در غلاف <i>Moringa oleifera</i> غربالگری شدند. نانوذرات مس از غلاف <i>Moringa oleifera</i> سنتز شدند و با استفاده از طیف‌سنج UV و FTIR و SEM مورد بررسی قرار گرفتند. فعالیت آنتی اکسیدانی نانوذرات مس نیز تعیین شد. دیسک‌های نانوذرات مس در غلظت‌های ۵۰ و ۱۰۰ میکروگرم بر میلی‌لیتر تهیه و برای اثر ضد میکروبی علیه اشريشياکلي، انتروکوكوس فکاليس، پنومونی کلبسیلا، استرپتوکوک اورئوس و کاندیدا آلبیکنس مورد آزمایش قرار گرفتند. فعالیت <i>E. coli</i> با تعیین لاکتات دهیدروژناز مورد سنجش قرار گرفت. نتایج: تجزیه و تحلیل طیف GCMS حضور Di-n-Octyl Phthalate و 2, 2-diethoxy Propane نشان داد. سنجش آنتی اکسیدانی خاصیت مهار رادیکال‌های آزاد را توسط نانوذرات مس نشان داد. طیف سنج UV سنتز نانوذرات مس را با نشان دادن جذب در ۲۲۰ نانومتر تایید کرد. بررسی SEM اندازه نانوذرات مس را در ۴۰ تا ۱۶۰ نانومتر نشان داد. تجزیه و تحلیل FTIR حضور گروه‌های OH و C=C را در نانوذرات مس نشان داد. کلبسیلا پنومونیه حساس‌ترین سویه به نانوذرات مس بود و پس از آن اشريشياکلي و کاندیدا آلبیکنس قرار داشتند. <i>E. coli</i> فعالیت لاکتات دهیدروژناز قابل توجهی را در دوز بالای نانوذرات مس نشان داد. نتیجه‌گیری: نانوذرات مس‌های سنتز شده از غلاف <i>Moringa oleifera</i> فعالیت ضد میکروبی قابل توجهی را در برابر میکروب‌ها نشان دادند.</p>	<p>گل‌وازگان:</p> <p>نانوذرات مس</p> <p>غلاف مورینگا اولیفرا</p> <p>فعالیت آنتی اکسیدانی</p> <p>منطقه بازدارندگی</p> <p>فعالیت ضد میکروبی</p>

مخلفات: CuONPs، نانوذرات مس؛ FTIR، طیف سنجی مادون قرمز تبدیل فوریه؛ SEM، میکروسکوپ الکترونی روبشی؛ LDH، لاکتات دهیدروژناز؛ GCMS، گاز کروماتوگرافی - طیف سنجی جرمی؛ NICM، مجموعه ملی میکروارگانیسم‌های صنعتی؛ NADH، نیکوتین آمید آدنین دی‌نوكلئوتید + (NAD) هیدروژن؛ DPPH، 2-دی‌فنیل-1-پیکریل‌هیدرازیل؛ NBT، نیترو آبی تترازولویوم؛ KBr، برミد پتاسیم

Sankar.m@rajalakshmi.edu.in, sankar7950@gmail.com, sankar7950.com *

تاریخ دریافت: ۲۶ اردیبهشت ۱۴۰۳؛ تاریخ دریافت اصلاحات: ۱۸ تیر ۱۴۰۳؛ تاریخ پذیرش: ۳۰ تیر ۱۴۰۳

doi: 10.61186/imp.23.89.17

© 2023. Open access. This article is distributed under the terms of the Creative Commons Attribution-NonCommercial 4.0 International License (<https://creativecommons.org/licenses/by-nc/4.0/>)